IOPscience iopscience.iop.org

Home Search Collections Journals About Contact us My IOPscience

# A theoretical analysis of quantum mechanical mixing of spin 1/2 with spin $^3/_2$ and admixed spin $^3/_2$-$^5/_2$ states in ferric haem complexes

This article has been downloaded from IOPscience. Please scroll down to see the full text article.

1994 J. Phys.: Condens. Matter 6 11071

(http://iopscience.iop.org/0953-8984/6/50/016)

View the table of contents for this issue, or go to the journal homepage for more

Download details:
IP Address: 171.66.16.179
The article was downloaded on 13/05/2010 at 11:34

Please note that terms and conditions apply.

J. Phys.: Condens. Matter 6 (1994) 11071–11080. Printed in the UK

# A theoretical analysis of quantum mechanical mixing of spin $\frac{1}{2}$ with spin $\frac{3}{2}$ and admixed spin $\frac{3}{2}$–$\frac{5}{2}$ states in ferric haem complexes

Archana Gupta and G P Gupta
Physics Department, Lucknow University, Lucknow 226007, India

Received 9 March 1994, in final form 22 August 1994

**Abstract.** The quantum mechanical admixture of spin $\frac{1}{2}$ and $\frac{3}{2}$ has been analysed theoretically. The analysis reveals that under the influence of the $S = \frac{1}{2}$ spin state, the Kramers doublets of $S = \frac{3}{2}$ split with $S_z = \pm\frac{3}{2}$ being the ground state in contrast to the case of the $S = \frac{5}{2}$ and $S = \frac{3}{2}$ admixture. The study of the mixing of spin $S = \frac{1}{2}$ with admixed spin $\frac{3}{2}$–$\frac{5}{2}$ states shows that when $S = \frac{1}{2}$ states are brought closer to the mixture, keeping the $\frac{5}{2}$–$\frac{3}{2}$ gap at a constant value, the two Kramers doublets of $S = \frac{3}{2}$ come closer to each other, cross over and become inverted. The effect of this crossover on the magnetic susceptibility and EPR signals is also discussed.

## 1. Introduction

Haem proteins are a class of biologically important macromolecules. In spite of the diverse functions, such as transportation of oxygen, reversible transfer of electrons and irreversible transformations of substrates, all haem proteins have the unifying feature of a common active site composed of an iron–porphyrin complex. Although the axial ligation to the haem group and the nature of the immediate environment are critical variables in modulating their enzymatic activity and biological control, it is believed that biological functions of haem proteins are determined to a large extent by the conformational and electronic properties of this haem group. Its versatility lies in the fact that the Fe ion can exist as $Fe^{2+}$, $Fe^{3+}$ and sometimes as $Fe^{4+}$ in a variety of crystal fields in high, low or intermediate spin configurations. A great deal of experimental and theoretical effort has been directed towards the elucidation of the detailed structure of the haem group. The close relation of the spin state to the structure made the investigation of spin states of considerable importance (Williams 1961, Hoard *et al* 1965, Hoard 1971, Scheidt and Reed 1981). Given the spin state of an Fe–porphyrin complex in either of its commonly occurring Fe (II) or Fe (III) oxidation states or with incompletely characterized states such as those of Fe (I) and Fe (IV), confident predictions about its structure can be made; e.g. the displacement of the Fe ion out of the porphyrin plane is linked with the spin state, the stereochemical 'trigger mechanism' of haemoglobin cooperativity. Magnetic susceptibility is one of the physical probes used to determine the electronic state at the haem site with the goal of relating the structure of the protein to its chemical function.

In the case of the ferric state the five d electrons can be arranged into three possible spin configurations—the low-spin ($S = \frac{1}{2}$) state, the intermediate-spin ($S = \frac{3}{2}$) state and the high-spin ($S = \frac{5}{2}$) state. The low- and high-spin states are well known and a number of examples of haem protein derivatives have been reported in which the Fe (III) atom is in

0953-8984/94/5011071+10$19.50 © 1994 IOP Publishing Ltd 

thermal equilibrium between the low- and high-spin states (Beetlestone and George 1961, Iizuka and Kotani 1968, 1969a, b, Iizuka *et al* 1968, 1971, Maltempo *et al* 1974, Scheidt *et al* 1982). However, the intermediate magnetic moments of bacterial haem proteins, known as the ferricytochromes c′, could not be explained on the basis of thermal equilibrium between the low- and high-spin states. The data could be interpreted in terms of a quantum mechanical admixture of the intermediate-spin state and the high-spin state (Maltempo 1974, Maltempo and Moss 1976). Since then, Mössbauer and susceptibility data of several synthetic haem complexes have been analysed using such an admixed spin $\frac{3}{2}$–$\frac{5}{2}$ state (Gupta *et al* 1986, 1987a, b, Scheidt *et al* 1989). Somehow the cases of quantum mechanical admixture of $S = \frac{1}{2}$ and $\frac{3}{2}$ have rarely been invoked as an explanation for experimental magnetic data of haem proteins (Gregson 1981). In this communication a theoretical study of the behaviour of a quantum mechanical admixture in ferric haem systems is presented with special reference to the $\frac{1}{2}$–$\frac{3}{2}$ state.

## 2. Theoretical formalism

The ground and low-lying excited states mix substantially via spin–orbit coupling to give spin mixed states. Such spin mixing gives rise to zero-field splitting, the magnitude of which is related to the strength of the spin–orbit coupling, the nature of the ground and the excited electronic states and their relative energies. The selection rules for the spin–orbit interaction between different haem Fe spin states are (i) $S = 0, \pm 1$, (ii) $S_z = 0, \pm 1$ (Griffith 1961). As a consequence the intermediate-spin state can mix quantum mechanically with the low-spin state as well as the high-spin state, precluding any possibility for the mixing of the high-spin state with the low-spin state. Besides this the mixing depends on the energy separation between unperturbed pure states. It can occur only if the energy separation is comparable to or less than the spin–orbit coupling constant (Salmeen and Palmer 1968).

In octahedral symmetry $O_h$ the five d orbitals are split into two sets of degenerate orbitals: the triply degenerate $t_{2g}$ orbitals ($d_{xy}$, $d_{xz}$, $d_{yz}$) and the doubly degenerate $e_g$ orbitals ($d_{x^2-y^2}$ and $d_{z^2}$). In ferric haem complexes the axial ligands lower the crystal field symmetry at the Fe site from $O_h$ to $C_{4v}$. For example in ferricytochromes c′ the symmetry at the Fe site is $C_{4v}$ and there is no magnetic evidence contrary to that (Maltempo 1974). The axial field corresponds to different ligand charge density in the $xy$ plane and along the $z$ axis and consequently splits both the $e_g$ and $t_{2g}$ orbital sets. The amount of $10Dq$ splitting and the loss of energy in violating Hund's rule of maximum spin can cause one of the $^6A_1$, $^4A_2$, $^4E$, $^4E$, $^2E$, $^2E$ and $^2B_2$ states to be the ground state. The electronic configurations of these energy levels are represented in figure 1.

In order to analyse the behaviour of quantum mechanical mixing of the above mentioned 24 states the eigenvalue problem was solved for the Hamiltonian

$$\mathcal{H} = \sum_{ij} \Delta_{ij} + \lambda \sum_i l_i \cdot s_i + \beta \sum_i (l_i + 2s_i) \cdot H \qquad (1)$$

with respect to a basis set consisting of 24 $|S_z\rangle$ components of the $^6A_1$, $^4A_2$, $^4E$, $^4E$, $^2B_2$, $^2E$ and $^2E$ states. The three terms in the Hamiltonian represent the crystal field, the spin–orbit and the Zeeman interactions respectively. The $\Delta_{ij}$ values are the energy gaps between different energy levels and may be introduced as free parameters along the diagonal elements corresponding to the respective energy states. $\lambda$ is the one-electron spin–orbit coupling constant and has been assumed to be equal to a usually accepted value of

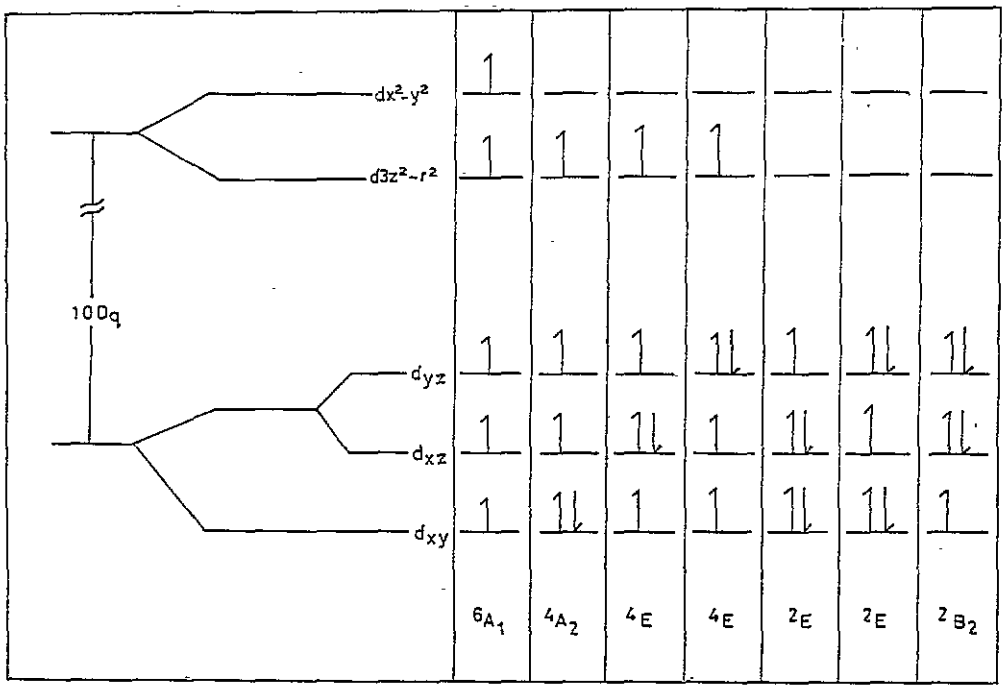


**Figure 1.** Electronic configurations of various energy levels of a ferric ion in the presence of an axially symmetric crystal field.

150 $cm^{-1}$ (Gupta *et al* 1986, 1987a, Scheidt *et al* 1989). An electrostatic energy term, which is constant for all the states, has been omitted from the expression. The $24 \times 24$ matrix elements of the Hamiltonian are generated from $10 \times 252$ Slater determinantal wave functions (Lang 1989) where 10 corresponds to the number of one-electron states in five d orbitals with spin up or spin down and 252 is the number of possibilities in which five electrons of $Fe^{3+}$ may be placed in the 10 one-electron states.

## 3. The interaction of $S = \frac{1}{2}$ with $S = \frac{3}{2}$

A careful examination of the matrix elements of the spin–orbit interaction term in the above mentioned basis set reveals that $^2B_2$ states do not interact directly with $^4A_2$ states. Nevertheless they interact with $^2E$ states, which directly mix with $^4A_2$ states. The matrix elements connecting $^2B_2$–$^2E$, $^2E$–$^2E$ and $^2E$–$^4A_2$ states are given in table 1. An exclusive interaction of $S = \frac{1}{2}$ with $S = \frac{3}{2}$ spin states was studied by keeping $^6A_1$ states very far ($\sim 90\,000$ $cm^{-1}$) from the ground state. Further, group theoretical methods indicate, and also by structural arguments it is evident, that only the $^4A_2$ quartet is stabilized in Fe porphyrins. This fact has also been established by fitting the susceptibility and Mössbauer data of a number of synthetic haem complexes (Gupta *et al* 1986, 1987a, b, Scheidt *et al* 1989). In view of these considerations and for the sake of simplicity both the $^4E$ states were also kept far away from the ground state ($\sim 90\,000$ $cm^{-1}$). Accordingly the interaction of all three doublets belonging to $S = \frac{1}{2}$, namely $^2B_2$, $^2E$ and $^2E$ only with the quartet $^4A_2$ was taken into consideration. The calculations were further simplified by considering the

**Table 1.** The matrix elements of the spin–orbit interaction operator $\sum l_i \cdot s_i$.

| | $\lvert^4A_2+\frac{3}{2}\rangle$ | $\lvert^4A_2+\frac{1}{2}\rangle$ | $\lvert^4A_2-\frac{1}{2}\rangle$ | $\lvert^4A_2-\frac{3}{2}\rangle$ |
|---|---|---|---|---|
| $\lvert^2E+\frac{1}{2}\rangle$ | $\frac{3}{2}$ | 0 | $\frac{1}{2}$ | 0 |
| $\lvert^2E-\frac{1}{2}\rangle$ | 0 | $\frac{1}{2}$ | 0 | $\frac{3}{2}$ |

| | $\lvert^2B_2+\frac{1}{2}\rangle$ | $\lvert^2B_2-\frac{1}{2}\rangle$ |
|---|---|---|
| $\lvert^2E+\frac{1}{2}\rangle$ | 0 | $\frac{1}{2}$ |
| $\lvert^2E-\frac{1}{2}\rangle$ | $\frac{1}{2}$ | 0 |

| | $\lvert^2E+\frac{1}{2}\rangle$ | $\lvert^2E-\frac{1}{2}\rangle$ |
|---|---|---|
| $\lvert^2E+\frac{1}{2}\rangle$ | $\frac{1}{2}$ | 0 |
| $\lvert^2E-\frac{1}{2}\rangle$ | 0 | $-\frac{1}{2}$ |

energy gap between the two $^2E$ states to be equal to zero, assuming the crystal field to be axially symmetric.

The mixing of $^2B_2$, $^2E$ and $^4A_2$ states was studied first by varying $\Delta_1$ keeping $\Delta_2$ constant, where $\Delta_1$ and $\Delta_2$ correspond to $^2B_2$–$^2E$ and $^2E$–$^4A_2$ energy gaps respectively. As shown in figure 2, when $\Delta_1$ was varied keeping $\Delta_2$ constant the position of $^2B_2$ states did not affect the splitting of other energy doublets significantly. However when $\Delta_1$ was kept constant and $\Delta_2$ was varied a large amount of mixing was observed. Figure 3 shows the changes in energy position of different Kramers doublets for $\Delta_2$ varying from $-1000$ cm$^{-1}$ to 1000 cm$^{-1}$ for a typical value of $\Delta_1 = 50$ cm$^{-1}$. As may be seen in figure 3, when $\Delta_2$ is large and negative all the doublets are nearly pure states with $^2E$ being the ground state. The two Kramers doublets $S_z = \pm\frac{1}{2}$ and $S_z = \pm\frac{3}{2}$, corresponding to $^4A_2$ states, are almost degenerate whereas the two $^2E$ doublets are not degenerate because of their mutual interactions. As the value of $\Delta_2$ is increased, all the states come closer to each other, their wave functions start mixing and finally for a large positive value of $\Delta_2$ the states become pure again but inverted, i.e. now $^4A_2$ becomes the ground state. The amount of mixing and the nature of the Kramers doublets can be ascertained by estimating the $g_\perp$ value of the ground state. As shown in figure 4, for large negative values of $\Delta_2$ the value of $g_\perp$ approaches 1.68, creeping towards two, the ideal value for $S = \frac{1}{2}$. As $\Delta_2$ is varied the value of $g_\perp$ decreases gradually and finally, for a large positive value of $\Delta_2$ it approaches zero, indicating that the Kramers doublet now belongs to $S_z = \pm\frac{3}{2}$. This point may be confirmed by estimating the $g_\perp$ value of the next Kramers doublet (shown as a dotted line in figure 4). It approaches the value of four, the ideal value corresponding to $S_z = \pm\frac{1}{2}$ belonging to $S = \frac{3}{2}$. It is interesting to note that when $^6A_1$ mixes quantum mechanically with $^4A_2$, $S_z = \pm\frac{1}{2}$ becomes the ground state in contrast to the present situation. This fact may be of significant importance in the interpretation of magnetic susceptibility data and EPR signals, and prompted more investigations as discussed below.

## 4. The interaction of $S = \frac{1}{2}$ with an $S = \frac{3}{2}$–$\frac{5}{2}$ admixture

Since the effect of $^2B_2$ on both $^2E$ and $^4A_2$ states was minimal as discussed above, the $^2B_2$ energy levels were taken far away from the ground state ($\sim 90\,000$ cm$^{-1}$) to facilitate the study of the combined effect of $^2E$ and $^6A_1$ on $^4A_2$ states. Calculations reveal that when $\Delta_2$, the gap between $^2E$ and $^4A_2$, is large as compared to $\Delta_3$, the gap between $^6A_1$ and $^4A_2$ states, the energy doublets of $^4A_2$ are split in accordance with the Maltempo model

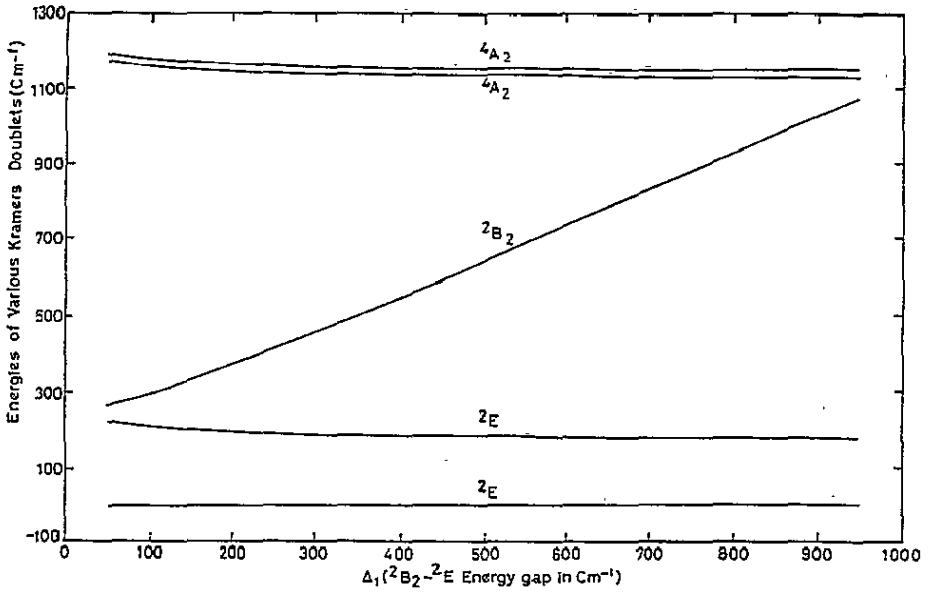


**Figure 2.** The energy eigenvalues for the $^4A_2$, $^2B_2$, $^2E$ and $^2E$ Kramers doublets plotted as a function of $\Delta_1$.

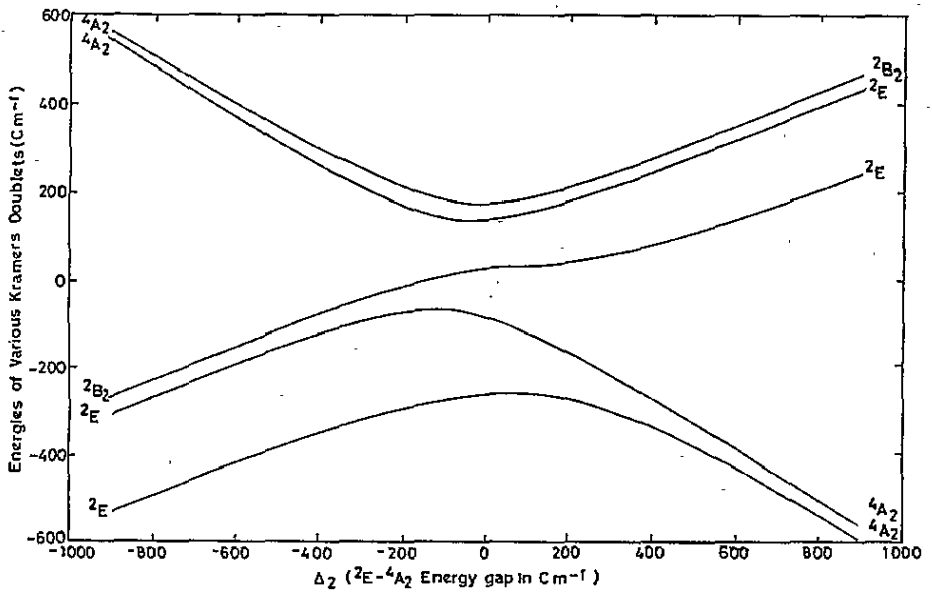


**Figure 3.** The energy eigenvalues for the $^4A_2$, $^2B_2$, $^2E$ and $^2E$ Kramers doublets plotted as a function of $\Delta_2$.

(Maltempo *et al* 1974, Maltempo and Moss 1976) i.e. $S_z = \pm\frac{1}{2}$ becomes the ground state. As $\Delta_2$ is decreased the two Kramers doublets of $^4A_2$ come closer to each other, cross over

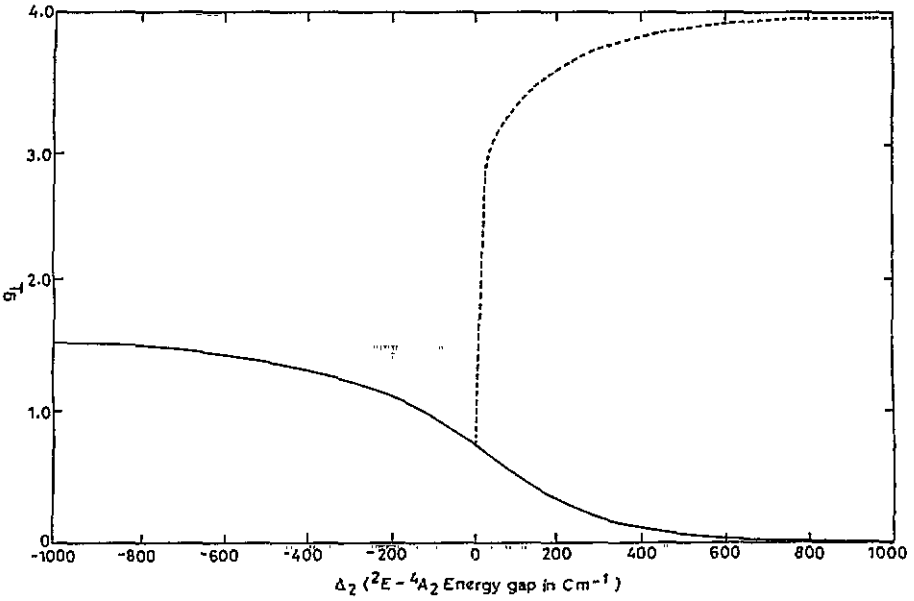


**Figure 4.** $g_\perp$ for the ground state Kramers doublet (solid line) and the next higher doublet (dotted line) plotted as a function of $\Delta_2$.

and are finally inverted i.e. $S_z = \pm\frac{3}{2}$ become the ground state. A typical behaviour of the two Kramers doublets as a function of $\Delta_2$ for $\Delta_3$ equal to an arbitrary value of 100 $cm^{-1}$ is shown in figure 5. The behaviour suggests that the effect of $S = \frac{1}{2}$ states on the quantum mechanical admixture of $S = \frac{3}{2}$ and $\frac{5}{2}$ increases exponentially when they are brought closer to the mixture. In order to understand the relative effect of $^2E$ and $^6A_1$ states on $^4A_2$ states the ratio $\Delta_2^*/\Delta_3^*$ was plotted as a function of $\Delta_3^*$ as shown in figure 6 where $\Delta_2^*$ and $\Delta_3^*$ are the critical values of $\Delta_2$ and $\Delta_3$ respectively for which the crossover of the two Kramers doublets of $^4A_2$ takes place. As may be seen in figure 6 the ratio $\Delta_2^*/\Delta_3^*$ increases exponentially for low values of $\Delta_3^*$, which means that even if $^6A_1$ is very close to $^4A_2$ its effect is negated by the distant $S = \frac{1}{2}$ spin states.

As has been mentioned above the crossover phenomenon may significantly affect the observed behaviour of EPR signals and the magnetic susceptibility of a system. In the case of the $S = \frac{3}{2}$–$\frac{5}{2}$ quantum mechanical admixed spin state, since the ground state Kramers doublet is $S_z = \pm\frac{1}{2}$ it provides strong EPR signals corresponding to both $g_\parallel$ and $g_\perp$ values. However, if $S = \frac{1}{2}$ spin states are close to the $S = \frac{3}{2}$–$\frac{5}{2}$ admixture such that $\Delta_2 < \Delta_2^*$ (for $\Delta_3 = \Delta_3^*$), the ground state is $S_z = \pm\frac{3}{2}$ and EPR signals corresponding to $g_\perp$ are reduced to zero. The cases of interest are under investigation and will be reported separately.

In order to see the effect of the crossover on the magnetic susceptibility a set of curves of $N_{\text{eff}}$, the effective Bohr magneton number, as a function of temperature, corresponding to the situations depicted in figure 5, are shown in figure 7. The values of $N_{\text{eff}}$ were calculated using the relation

$$N_{\text{eff}} = \sqrt{-3kTg\langle S\rangle/H\beta} \tag{2}$$

and the powder average was estimated using the relation

$$N_{\text{eff}} = \tfrac{1}{3}N_{\text{eff}}(\parallel) + \tfrac{2}{3}N_{\text{eff}}(\perp). \tag{3}$$

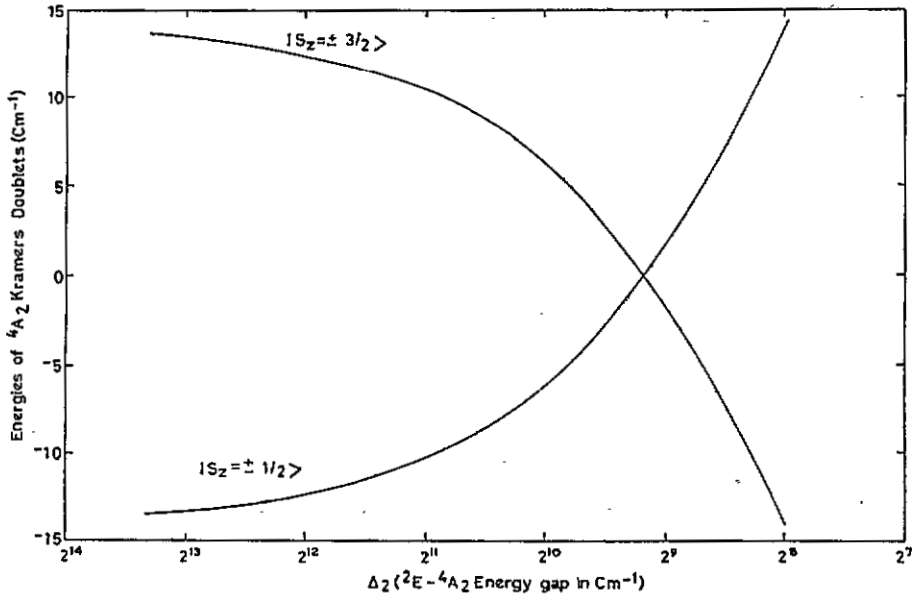


**Figure 5.** The energies of the two Kramers doublets of $^4A_2$ plotted as a function of $\Delta_2$ for $\Delta_3 = 100\ cm^{-1}$.

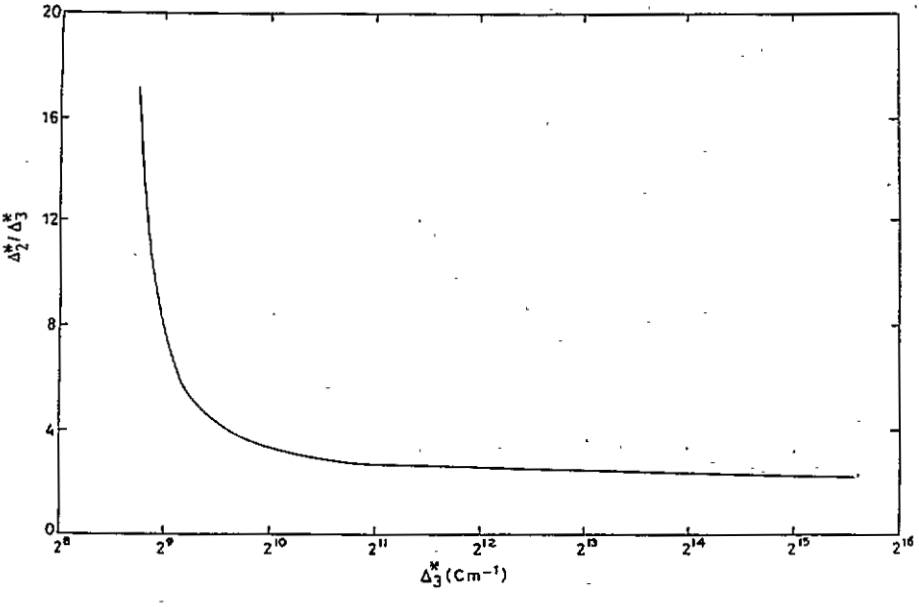


**Figure 6.** $\Delta_2^*/\Delta_3^*$ plotted as a function of $\Delta_3^*$.

As shown in figure 7, at low temperatures, where crystal field effects are dominant, values of $N_{eff}$ increase as $\Delta_2$ is decreased from 800 $cm^{-1}$ to 500 $cm^{-1}$ (shown as dotted

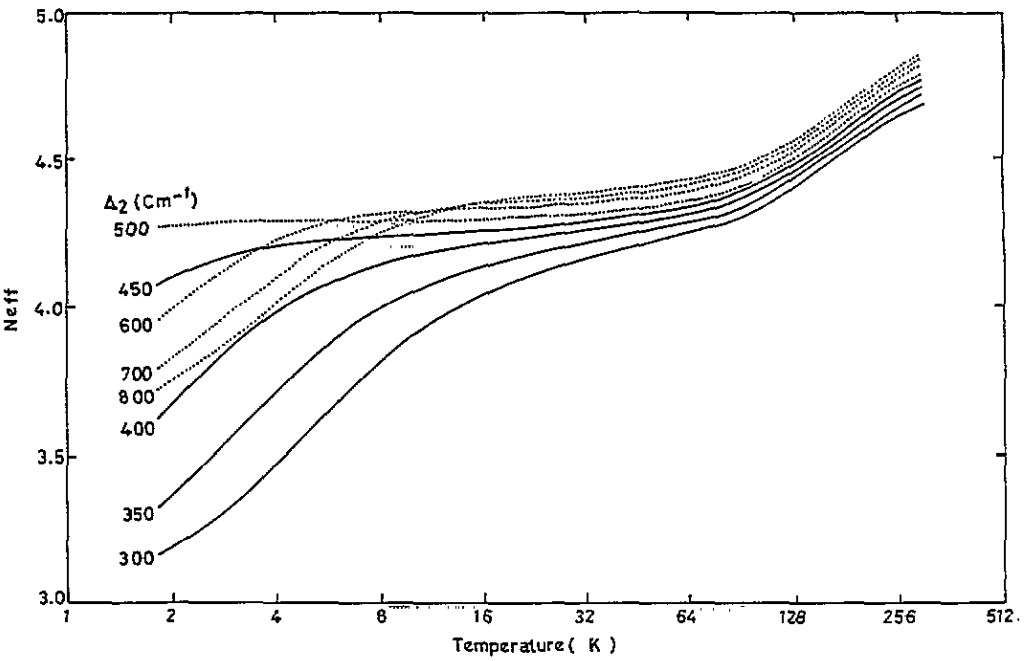


**Figure 7.** *The values of $N_{eff}$ plotted as a function of temperature for different values of $\Delta_2$ and a fixed value of $\Delta_3 = 100$ cm$^{-1}$.*

curves). For $\Delta_2 = 500$ cm$^{-1}$ the curve becomes approximately a straight line parallel to the temperature axis. This corresponds to the situation when the crossover is taking place and the two Kramers doublets are almost degenerate. The susceptibility behaviour is quite close to that obtained from the Curie law. When $\Delta_2$ is decreased further from 500 cm$^{-1}$ to 300 cm$^{-1}$ the low-temperature part of the curve moves downward again but at a faster rate (shown by the solid curves). This is conceivable in view of the fact that now $S_z = \pm\frac{3}{2}$ becomes the ground state and does not contribute to the perpendicular susceptibility of the system.

In a number of cases reported in the literature the low values of $N_{eff}$ at low temperature and the weak EPR signals have been interpreted in terms of a dimer type of weak antiferromagnetic coupling. It may be interesting to investigate whether both observations are due to the presence of $S = \frac{1}{2}$ spin states in the vicinity.

As an example, the susceptibility data of [Fe(OEP)(3-ClPy)]$ClO_4$ (OEP = octaethylporphyrinate) had been interpreted in terms of a quantum mechanical mixture of spin $\frac{3}{2}$ and $\frac{5}{2}$ only. The deviation of the theoretical curve from the experimental data, which started from $\sim$ 130 K, was attributed to the dimer type of antiferromagnetic coupling (Gupta *et al* 1986). A preliminary fitting of these data by taking into account $^2$E states along with an $S = \frac{3}{2}$ and $\frac{5}{2}$ admixture is shown in figure 8. The calculated values match well with the experimental ones for $\Delta_2 = 410$ cm$^{-1}$, $\Delta_3 = 260$ cm$^{-1}$ and $\lambda = 135$ cm$^{-1}$. As may be seen in figure 8, the theoretical curve deviates from the data only below $\sim$ 10 K. This suggests that the antiferromagnetic coupling present in the dimers may be much smaller than the previously reported value, which might have been estimated too high as $^2$E states had been ignored. The other important point is that the ground state in this case is $S_z = \pm\frac{3}{2}$

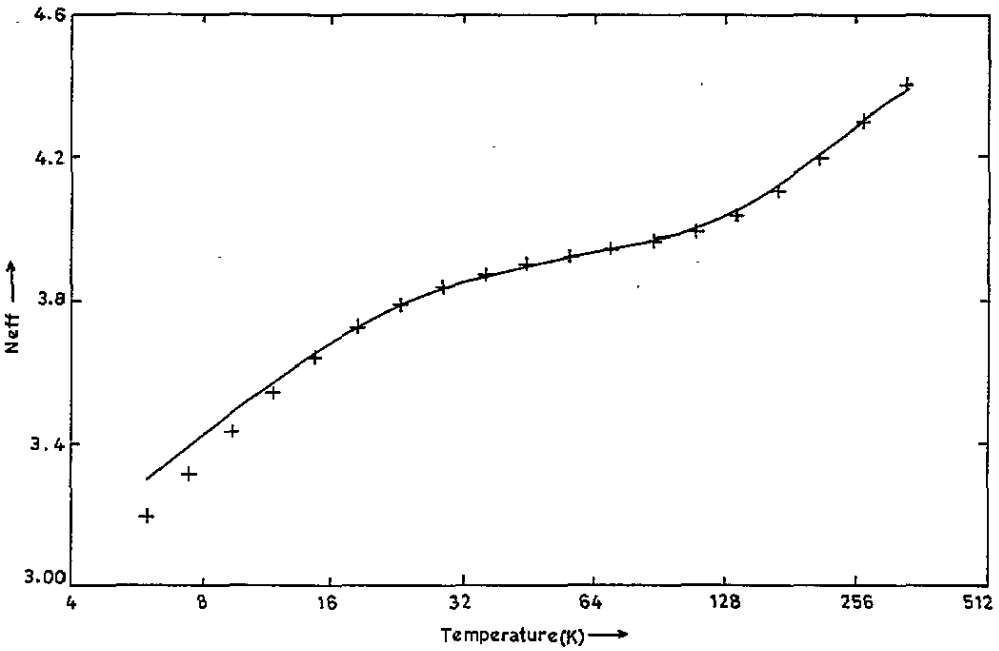


**Figure 8.** The experimental values of $N_{eff}$ (+) for the complex [Fe(OEP)(3-ClPy)]$ClO_4$ plotted as a function of temperature. The solid curve corresponds to the theoretical values. The data have been multiplied by a factor of 0.95 to compare with the most suitable curve. The factor is well within experimental error (Gupta *et al* 1985).

rather than $S_z = \pm\frac{1}{2}$. As mentioned earlier, this point may play an important role in the interpretation of EPR and Mössbauer data. A detailed analysis of this and other complexes is under investigation at present and will be reported separately.

## Acknowledgment

One of the authors (AG) is grateful to the Council of Scientific and Industrial Research for financial assistance.

## References

Beetlestone J and George P 1961 *Biochemistry* **3** 707
Gregson A K 1981 *Inorg. Chem.* **20** 81
Griffith J S 1961 *The Theory of Transition Metal Ions* (Cambridge: Cambridge University Press)
Gupta G P, Lang G, Lee Y J, Scheidt W R, Shelly K and Reed C A 1987a *Inorg. Chem.* **26** 3022
Gupta G P, Lang G, Reed C A, Shelly K and Scheidt W R 1987b *J. Chem. Phys.* **86** 5288
Gupta G P, Lang G, Scheidt W R, Geiger D K and Reed C A 1985 *J. Chem. Phys.* **83** 5945
—— 1986 *J. Chem. Phys.* **85** 5212
Hoard J L 1971 *Science* **174** 1295
Hoard J L, Hamor M J, Hamor T A and Caughey W S 1965 *J. Am. Chem. Soc.* **87** 2312
Iizuka T and Kotani M 1968 *Biochim. Biophys. Acta* **154** 417
—— 1969a *Biochim. Biophys. Acta* **181** 275

Iizuka T and Kotani M 1969b *Biochim. Biophys. Acta* **194** 351
Iizuka T, Kotani M and Yonetani T 1968 *Biochim. Biophys. Acta* **167** 257
—— 1971 *J. Biol. Chem.* **246** 4731
Lang G 1989 Private communication
Maltempo M M 1974 *J. Chem. Phys.* **61** 2540
Maltempo M M and Moss T H 1976 *Q. Rev. Biophys.* **9** 181
Maltempo M M, Moss T H and Cusanovich M A 1974 *Biochim. Biophys. Acta* **342** 290
Salmeen I and Palmer G 1968 *J. Chem. Phys.* **48** 2049
Scheidt W R, Geiger D K and Haller K J 1982 *J. Am. Chem. Soc.* **104** 495
Scheidt W R, Osvath S R, Lee Y J, Reed C A, Shaevitz B and Gupta G P 1989 *Inorg. Chem.* **28** 1591
Scheidt W R and Reed C A 1981 *Chem. Rev.* **81** 543
Williams R J P 1961 *Fed. Proc. Fed. Am. Soc. Exp. Biol.* **20** 5